



Numerical Research on the Impact of Axial Position of Endwall Suction Slot on Tip Leakage Flow

B. Zhang, B. Liu[†], A. Rehman and X. Sun

School of Power and Energy, Northwestern Polytechnical University, Xi'an, Shaanxi, 710072, P. R. China

[†]Corresponding Author Email: liubo704@nwpu.edu.cn

(Received October 29, 2019; accepted December 31, 2019)

ABSTRACT

In order to reduce the adverse effect of the tip leakage flow of cantilever stator on compressor performance, the impact of the axial position of endwall streamwise suction slot on tip leakage flow was numerically studied. The study on the overall performance of the compressor and the details of the flow field near the stator end region with and without suction showed that all suction schemes could weaken the tip leakage flow intensity to a certain extent, and the flow control effect was gradually enhanced with the increase of the suction flow rate. In the case of small suction flow rate, for example, 0.5%, the short slot schemes can improve the overall efficiency of the compressor by about 0.5%, which is more advantageous than the long slot scheme, and the overall efficiency improvement of the latter is about 0.3%. The advantage of the long slot scheme in flow control is reflected in the case of large suction flow rate, that is, 1.0%, which may improve the overall efficiency of the compressor by about 0.96%. The axial position of suction slot has a significant influence on flow control effect of the tip leakage flow. Compared with the downstream suction, which only modified the flow field by reducing the blocking effect generated by tip flow vortex, the upstream suction could better control the tip leakage flow by restraining the development of the initial stage of the leakage vortex. Besides, the endwall suction scheme with a full chord length slot has the greatest impact on the passage vortex, its effect on modifying the flow field near the end zone was determined by the combinatorial action of the enhancement of the passage vortex and the attenuation of the leakage vortex.

Keywords: Cantilever Stator; Tip Leakage Flow; Endwall Suction; Suction Position; Passage Vortex; Blocking effect.

NOMENCLATURE

BLS	Boundary Layer Suction	SU	Upstream short slot suction scheme
BTS	Blade Tip Suction	SV	Separation Vortex
Cp	Static pressure coefficients	TE	Trailing Edge
ES	Endwall Suction	TLF	Tip Leakage Flow
Hn	normalized helicity	TLV	Tip Leakage Vortex
LB	suction scheme with long slot	u_{ij}	components of a vector field
LE	Leading Edge	W	relative flow velocity
NS	Near Stall	y+	non-dimensional wall distance
PE	Peak Efficiency	η^*	isentropic efficiency
PS	Pressure Surface	σ^*	total pressure recovery coefficient
PV	Passage Vortex	π^*	total pressure ratio
Q	vortex determination criterion	Ψ	normalized flow coefficient
S_{ij}	strain-rate tensor	ω	absolute vorticity
SD	Downstream short slot suction scheme	Ω_{ij}	spin tensor
SS	Suction Surface		
SFR	Suction Flow Rate		

1. INTRODUCTION

With the development of the smart high performance engines having high load and high total pressure ratio, the blades of the compressors have to work under larger transverse pressure gradients. This may tend to aggravate the flow separation on the endwall and blade surfaces and reduce the efficiency and stability margin of compressor. It is well known that a large transverse pressure gradient also enhances the intensity of the tip leakage flow (TLF), which further complicates the flow field due to the interaction of the leakage flow, endwall boundary layer flow, main flow, and shock wave for transonic fans and compressors. The blocking effect in the end zone and the total pressure loss caused by the TLF may increase, resulting in a decrease in compressor aerodynamic performance (Denton 1993; Suder 1998). Therefore, it is particularly important to control and modify the flow field near the clearance to improve the aerodynamic performance and increase the stable operating range of the compressor.

Driven by the pressure difference between the suction surface (SS) and the pressure surface (PS) of the blade, the TLF rolls up to form the tip leakage vortex (TLV) and interacts with the mainstream flow and the end wall boundary layer. Kang and Hirsch *et al.* (1994), based on the experimental results, proposed a three-eddy model of tip clearance leakage flow field, which consisted of the TLV, tip separation vortex (SV) and secondary vortex. The results of some pieces of literature showed that the performance of compressor and cascade could be improved as the separation flow was controlled by introducing an appropriate clearance size. While a larger clearance size led to the enhancement of the TLF, which would decrease the performance of the compressor (Zuo *et al.* 2011; Chen *et al.* 2012, 2013; Gottschall *et al.* 2012; Gao *et al.* 2017). In addition, Liu *et al.* (2016a) and Mao *et al.* (2019) explored the effect of tip clearance of the rotors on the performance of a counter-rotating axial flow compressor. It was shown that with the increase of tip clearance, the onset location of TLV was shifted downstream, and the efficiency and total pressure ratio of the compressor decreased. Meanwhile, the sensitivity of the influence of leakage flow of the other rotor whose clearance was not changed to the clearance change of the front and rear rotor was different, and the change of the rear rotor showed a more significant impact on the front rotor.

The unsteady characteristics of clearance leakage flow may also cause compressor rotating stall, which will have a very adverse impact on compressor performance. At present, it is considered that the self-induced unsteadiness (Du *et al.* 2010), vortex splitting and vortex breakdown (Liu *et al.* 2016b; An *et al.* 2018; Wu *et al.* 2019), are the main reasons of stall initiation mechanism, and a lot of work has been done (Vo *et al.* 2008).

Because of the blockage of flow field in the end region due to the TLF and TLV near clearance,

which has adverse effects on the total pressure ratio, the efficiency and the stall margin, various flow control methods have been developed to the TLF and the TLV to modify the flow field near blade tip region. The boundary layer suction (BLS) has attracted much attention due to its high efficiency, practicability and great application prospects in flow control. The BLS technology was applied to the surface of compressor stator blade by Loughery *et al.* (1971), which greatly enhanced the ability of airflow turning and efficiency of the compressor. Subsequently, a large number of numerical and experimental studies showed that the application of BLS technique could effectively control boundary layer separation of the blade SS and corner (Guo *et al.* 2010; Shi *et al.* 2015a). Lu *et al.* (2016) inhibited the development of the TLF and TLV of a compressor cascade with gap by using the blade tip suction scheme (BTS) because the onset position of TLV shifted downstream.

Similarly, the research on compressor cascade by Mao *et al.* (2018a) also showed that the BTS has an inhibitory effect on the TLF and TLV, and the optimal axial location of the suction slot should be located in the development region of TLV. Cao (2014) studied the influence of the circumferential position of the endwall suction (ES) slot in flow direction on the TLF through a compressor cascade with clearance. The results showed that the flow control effect was the best when the suction slot was positioned directly above the blade tip, and the flow control effect increased with the increase of suction flow rate (SFR, defined as the ratio of the suction mass flow rate to the inlet mass flow rate.). Some scholars have also studied the flow control of the TLF by slotting or grooving suction on the rotor casing and had a better understanding of the mechanism of BLS to suppress the TLF and TLV (Gümmer *et al.* 2008; Lu *et al.* 2017a; Perry *et al.* 2017; Mao *et al.* 2017, 2018b).

In above studies, the flow control of the TLF and TLV by BLS was mostly focused on slotting along the blade tip or opening circumferential slots on the rotor casing, while the suction slot on endwall was mainly focused on the cascade flow field rather than real compressors. Because of the difference between the actual flow field of compressor and cascade, it is necessary to study the flow control effect of endwall suction on compressor performance. Understanding the role of the axial position of the suction slot in controlling the tip leakage flow is of great significance to the practical application of the aspiration technique in compressors.

In this paper, an axial single-stage transonic compressor was numerically simulated to study the flow control mechanism of the endwall suction scheme along flow direction on the tip leakage flow of the cantilever stator. The effect of the axial position of suction slot on the modification of the compressor flow field with endwall suction schemes was focused in this study. This paper is organized as follows. Firstly, the compressor stage and the design of aspiration schemes are introduced in section 2.1 and 2.2, respectively. Then, the numerical method

and validation are presented in section 3. Subsequently, the numerical results and discussion are presented in section 4, and a list of conclusions is finally summarized in section 5.

2. INVESTIGATED COMPRESSOR AND THE DESIGN OF ENDWALL SUCTION SLOTS

2.1 Investigated Compressor Stage

The test case in this paper is the axial single-stage transonic compressor, NASA Stage 35, which consists of a row of rotor blades and a row of stator blades. The main design parameters are listed in Table 1. The calculation domain diagram of the compressor is shown as Fig.1. In order to study the effect of the endwall suction scheme on the TLF of cantilever stator, the clearance size of stator blade is set to 0.8 mm, which is about 2% chord of the stator blade tip. This is also within the reasonable gap size of most actual cantilever stators. It should be noted that the description of cantilever stator tip in this paper refers to the clearance end near the hub of stator blade. All expressions of relative blade height in this paper were based on the hub plane.

Table 1 Design parameters of the compressor

parameters	values
Rotational speed (r/min)	-17188.7
Rotor blades count	36
Stator blades count	46
Rotor aspect ratio	1.19
Stator aspect ratio	1.26
Hub-tip radius ratio	0.7
Design tip speed (m/s)	454
Design pressure ratio	1.82
Design conversion flow (kg/s)	20.188

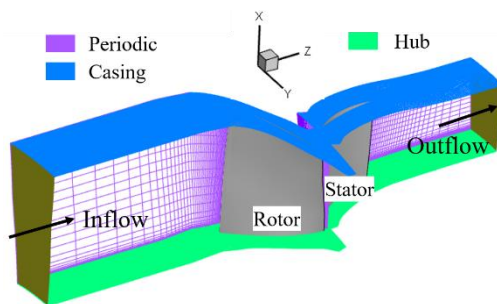


Fig. 1. Structure of the axial single-stage transonic compressor.

The AutoGrid5 from NUMECA International was used to generate a single-channel O4H mesh topology. The “butterfly grid” technology was adopted to ensure the mesh quality near the clearance region. There were 17, 21 and 173 mesh nodes arranged in the inner layer of the butterfly grid along the I, J and K directions, while there were 13, 21 and 309 mesh nodes in the outer layer. The minimum grid spacing of the first layer of walls was set to be

$1 \times 10^{-6}m$ so that the non-dimensional wall distance $y^+ < 3$, which was satisfied with the applicable condition of the turbulence model used in current research. The influence of grid number on the calculation results was given as Fig.2. When the total number of grids exceeded 1.95 million, the calculation results of the compressor efficiency and total pressure ratio changed little with the increase of grid density. Accordingly, combining the findings of Lin *et al.* (2019), the total number of mesh nodes of the computational grid was set to about 2.0 million. Figure 3 shows the computational grid schematic diagram of the SS of rotor blade and the PS of stator blade as well as the hub surface, meanwhile the enlarged local grid of the leading and trailing edges (LE, TE) of the stator blade tip is also given.

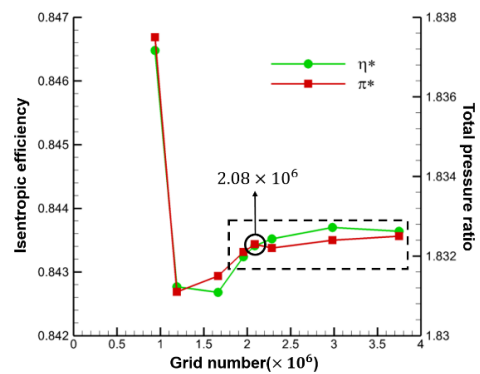


Fig. 2. Compressor performance with different number of meshes.

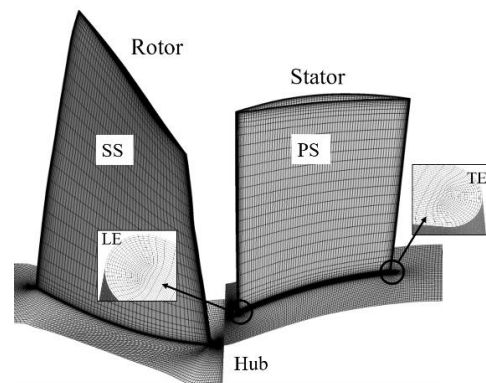


Fig. 3. Computational mesh of compressor and local enlargement of mesh at the stator blade tip.

2.2 Design of Suction Slots

In order to investigate the flow control effect of ES on tip leakage flow in cantilever stator of the compressor, the flow field of the original compressor with and without suction was compared. Three endwall aspiration schemes were designed to study the flow control effect of the axial position of the suction slot along flow direction on the clearance leakage flow and leakage vortex. The schematic diagram of three schemes is shown in Fig.4. Here, the slot setting of the flow control scheme on hub corner separation was referred to Cao (2014).

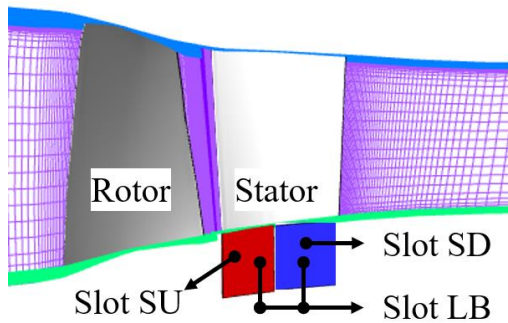


Fig. 4. Schematic diagram of schemes of the endwall suction slot.

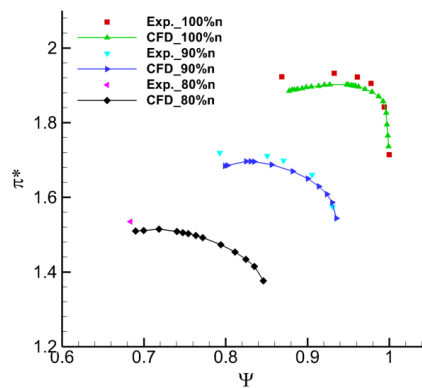
The suction slots were located on the hub endwall and paralleled to the suction surface profile of stator blade tip, which could control the corner separation phenomenon under the large incidence angle. In addition, the width of the suction slots was 1.5mm and the height was 10mm. The suction scheme called Slot SU was located upstream of clearance, the Slot SD scheme was located downstream of clearance, and the Slot LB scheme covered whole chord length range of the stator blade tip. The IGG from NUMECA International was used to generate an H-type topology for slot grids. The number of grid nodes in the direction of I, J and K of the short slots was 45, 61 and 29, respectively, thereby the total number of nodes of these slots was about 80,000, while that of the long slot was about 160,000. The suction slot mesh was connected with the mesh of stator passage by using the full non-matching connecting technique to ensure that there was no obvious loss in the numerical transfer process.

3. NUMERICAL METHODOLOGY AND VALIDATION

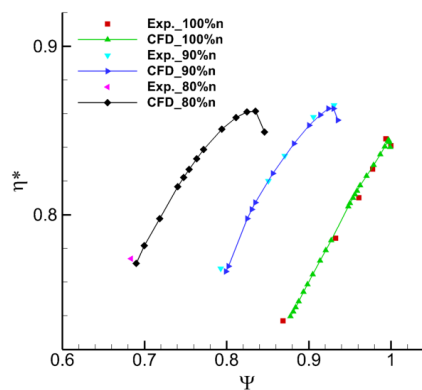
The numerical calculation was based on the steady simulation by using Fine/Turbo from NUMECA International to solve the compressible three-dimensional Reynolds-averaged Navier-Stokes equations. According to the literature of *Glanville et al.* (2001) and *Lee et al.* (2004), the Spalart-Allmaras (S-A) turbulence model could agree well in predicting the location, trajectory, and loss of TLV. Moreover, its convergence and stability of the model are better than those of two-equation turbulence models in the calculation of the clearance leakage flow using suction technology. Therefore, under the guidance for the selection of turbulence model in NASA Stage35 compressor by *Lin et al.* (2019), considering the time cost and accuracy of the calculation, the S-A turbulence model of low-Re models was chosen for accurate calculation. The cell-centered finite volume scheme was implemented, and the fourth-order Runge-Kutta scheme was used to discretize the time term of equations. The CFL value was given as 3.0, and the multi-grid acceleration technique and implicit residual smoothing method were used to accelerate convergence. The inlet boundary conditions were imposed based on total temperature, total pressure

and inlet flow angle. At the outlet of the compressor passage, the average static pressure was imposed. The mass flow rate of suction flow and the initial backpressure were given as the outlet condition of suction slot. In addition, adiabatic and non-slip boundary conditions were applied on solid walls.

In order to validate the effectiveness of the calculation method adopted in the present work, the compressor aerodynamic performance curves calculated by numerical calculation at 100%, 90% and 80% design rotating speed were compared with the experimental results (*Reid et al.* 1978) as shown in Fig.5. The abbreviation ‘‘CFD’’ denotes the results of numerical simulation and ‘‘Exp.’’ denotes the experimental results. The mass flow rates are all normalized with the blocking mass flow rate. Compared with the experimental results, the total pressure ratio obtained by numerical calculation was somehow lower under all working conditions except near choke, which may be due to the difference between numerical and experimental data processing methods (*Denton 1997*) and the differences in model settings. However, the prediction of choke and stall points was much accurate and the overall distribution trends of total pressure ratio and isentropic efficiency were in good agreement.



(a) Total pressure ratio



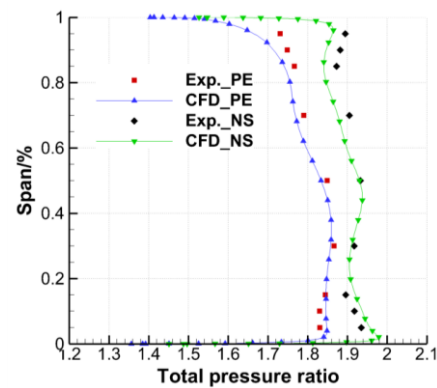
(b) Isentropic efficiency

Fig. 5. Characteristic comparison of results of experiment and calculation.

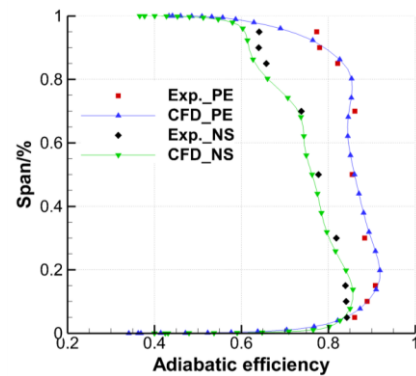
Figure 6 shows the comparison of radial distributions at outlet between the numerical and experimental

results drawn by calculating the circumferential mass-averaged total pressure ratio and adiabatic efficiency of the compressor at design rotating speed at peak efficiency point and near stall point. It can be seen that there were some differences between the calculated results and the experimental values near the casing due to the overestimation of the loss model, but they were almost identical near the low span spread, and the overall distribution trend was basically the same. Figure 7 shows the details of the comparison of experimental (Van Zante *et al.* 2000) and numerical absolute tangential velocity at 33% and 92% rotor chord slices at the design speed near the PE. The areas with higher tangential velocity are mainly concentrated in the area near the blade tip, and the corresponding position is the area of the tip leakage flow. By comparison, it can be seen that the position of the TLF corresponding to the numerical results is basically consistent with the experimental results, and the low tangential velocity region near the blade SS is basically the same as the experimental results. The numerical method has high reliability for the capture of the flow field details in the rotor passage. Therefore, the prediction of the hub leakage flow in the stator should also be credible.

Therefore, the consistency between numerical simulation and experimental results gave us reason to believe that the research and conclusions obtained by using this numerical method were credible and trustworthy.



(a) Total pressure ratio



(b) Adiabatic efficiency

Fig. 6. Distribution of total pressure ratio and adiabatic efficiency along radial direction under peak efficiency and near stall conditions.

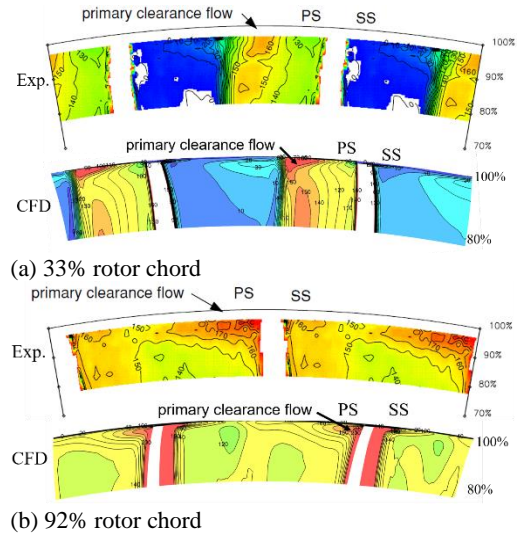


Fig.7. Comparison of tangential velocity distribution at different axial slices near the peak efficiency point at design rotating speed.

4. RESULTS AND DISCUSSION

4.1 Effect of the Endwall Suction on the Compressor Performance and Tip Leakage Flow

Due to the large difference between the mass flow of the suction and non-suction compressor under the same boundary condition at the near stall point and peak efficiency point (near choke), it is impossible to guarantee that the change of the flow field is only caused by the introduction of suction. Therefore, in this paper, 97.2% blocking mass flow rate was taken as a normal condition that the difference of mass flow was not obvious before and after suction to study the flow control effect of the endwall suction scheme on the tip leakage flow in the stator clearance and its flow control mechanism.

The isentropic efficiency of the compressor and the total pressure recovery coefficient of the stator varied with suction flow rate under three suction schemes is shown in Fig.8. From the figure, it could be seen that the isentropic efficiency of the compressor of three suction schemes has been improved, and the efficiency increased gradually with the increase of SFR. The change rule of the total pressure recovery coefficient of the stator with SFR is same as that of the isentropic efficiency. The endwall suction reduced the leakage loss and the blending loss among the leakage flow, the endwall boundary layer and the main flow by sucking out low-energy fluids such as the TLF, thereby increasing the isentropic efficiency of the compressor. Compared with three suction schemes, the two short slot suction schemes were more advantageous to improve efficiency representing the compressor total performance than the full chord slot suction scheme while the SFR was small. At the condition of the SFR of 0.5%, the isentropic efficiency of the short slot suction schemes was increased by about 0.5% than that of the original, while that of the long slot scheme was

increased by about 0.3%. The reason for this difference was the greater interference effect of the long slot on the flow field near the endwall region than that of the short slot schemes. Although the compressor efficiency of the upstream and downstream endwall suction schemes was basically equal at the SFR of 0.5%, the total static pressure recovery coefficient of the upstream suction scheme is larger, reflecting the improvement effect of the upstream suction scheme on the compressor was better than downstream endwall suction scheme.

The advantages of the long slot suction scheme in improving compressor performance were fully reflected as the SFR was large, and the isentropic efficiency could be improved up to about 0.96% when the SFR was 1.0%. At the same time, the total pressure recovery coefficient was also the biggest improvement over the prototype compressor stator. With the increase of the total pressure recovery coefficient of the stator, the total pressure ratio of the compressor also increased under the premise that the rotor's working condition was unchanged. Therefore, the long slot suction scheme had a tendency to better improve the compressor performance under a large suction flow rate. However, considering the structural strength and the cost of air entrainment, short slot suction scheme and smaller suction flow are the goals we want to pursue.

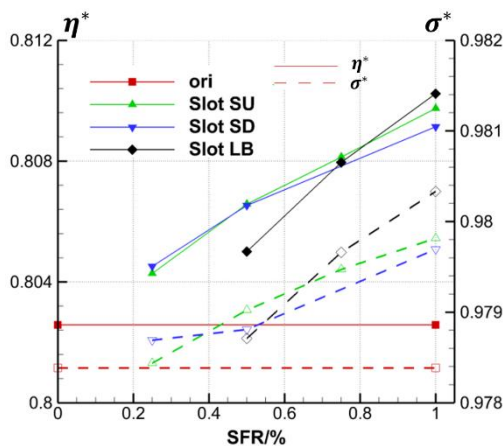


Fig. 8. Trend of the isentropic efficiency of the compressor and the total pressure recovery coefficient of the stator with suction flow rate.

According to the research viewpoints of Storer and Inoue *et al.* (Storer *et al.* 1990; Inoue *et al.* 1989, 1998), the trajectory of leakage vortex near the stator blade tip coincided with the line of the inclined channel connecting the local minimum static pressure on hub endwall. In addition, the minimum static pressure point on the hub endwall was considered as the onset position of leakage vortex. The isolines of static pressure coefficients (C_p) on the hub endwall for three different suction schemes was shown as Fig.9, in which the static pressure coefficient was defined as the ratio of the local pressure to inlet total pressure. The red dotted arrows in the figure were the lines connected with the local minimum hydrostatic coefficients, representing the trajectories of the tip leakage vortex.

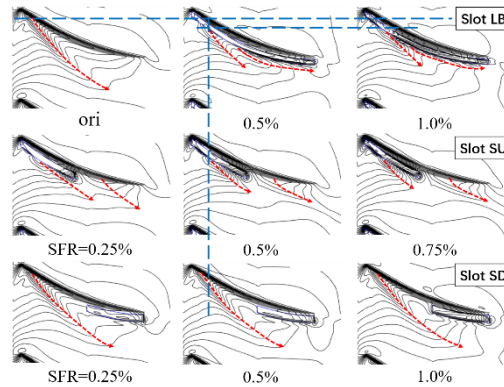


Fig. 9. Static pressure coefficient isolines on the hub endwall.

It could be seen from the figure that three suction schemes had changed the motion of the TLV. With suction by the Slot LB and Slot SU schemes, the number of the trajectory of TLV changed from one to two, whose onset points started near the stator blade LE and at the middle chord, respectively. By analyzing the Slot LB scheme, the onset position of the TLV moved downstream with the increase of SFR, the track of TLV starting from the blade LE approached the stator blade SS, meanwhile, the axial development distance became shorter. The onset position of the TLV that started at the middle chord did not change with the increase of the SFR, but the circumferential influence range decreased gradually. The Slot SU and Slot LB schemes had the same trajectory of TLV started near the stator blade LE, the onset position of this part TLV moved downstream refer to original, and the trajectory of TLV was closer to the SS of stator blade. In addition, the onset position of the TLV at the middle chord under the Slot SU scheme was closer to the TE of the blade but the circumferential influence range was larger than that of the scheme Slot LB. With suction by the Slot SD scheme, the trajectory of TLV did not change significantly, but only approached the stator blade SS with a large SFR.

These phenomena indicated that the endwall suction could weaken the leakage vortex strength and reduce the influence range of the TLF and TLV. Through the change of the onset position of the TLV in the three endwall suction schemes with the suction flow rate of 0.5%, one could clearly see that the starting point of the TLV of the Slot SD scheme was the nearest from the blade LE, so it had the worst flow control effect on the TLF and TLV. Referring to Fig.8, the isentropic efficiency of the Slot SU scheme was higher than that of the Slot LB scheme, which seemed to indicate that the onset position of leakage vortex had a greater influence on the flow field in the tip region than the distance between the trajectory and the suction surface of the blade.

4.2 Influence of the Axial Position of the Endwall Suction Slot on the Tip Leakage Flow

Taking the operating condition with suction flow rate of 0.5% as an example, the effects of three suction

schemes on the leakage flow of cantilever stator were analyzed. Firstly, the three-dimensional streamlines of the leakage flow in the stator mid-gap of the original and suction schemes were shown as Fig.10. The local Mach number showed the color of the leakage streamlines. It could be seen from the figure that the three-dimensional streamlines of the TLV were partially absorbed by suction slots, whose region was marked by the black ellipse in the figure of each endwall suction scheme. Meanwhile, the streamlines were obviously close to the SS of the stator blade, indicating that the intensity of the TLF was obviously weakened. Nevertheless, compared with the changes of streamline structure and location, the flow control effect of each suction scheme on the TLF and TLV was different.

The winding structure of the three-dimensional streamlines near the stator blade LE of the Slot LB scheme was weakened and simple, marked with the red dotted, and the direction of the TLF at the outlet was almost as same as that of the mainstream. The winding structure of the Slot SU scheme was almost invisible, but this suction scheme had little influence on the downstream leakage flow behind the suction slot. While the slot SD scheme had no effect on the leakage flow near the blade LE, but mainly controlled the leakage flow near the TE of stator blade. It was also found intuitively that Slot LB scheme had the most obvious control effect on the trajectory of leakage flow with the same SFR, which corresponded to the previous analysis. In addition, the leakage flow in the downstream part of the suction slot was more affected than that in the upstream part due to the gradual increase of the pressure difference between the inlet and outlet of the suction slot along the flow direction.

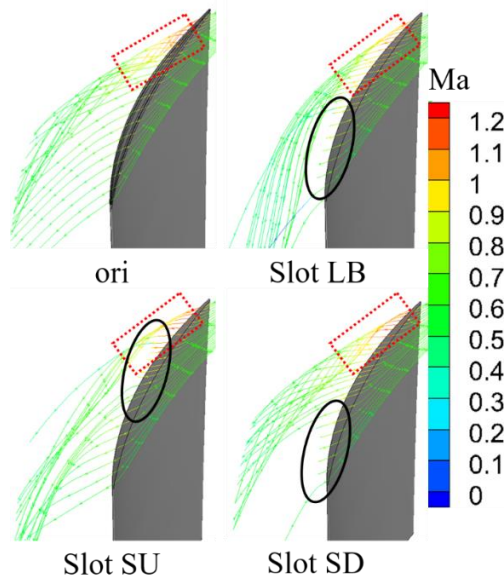


Fig. 10. Three-dimensional streamlines of leakage flow with the suction flow rate of 0.5%.

Then, Fig.11 shows the two-dimensional streamlines and entropy contours near the hub endwall region on

S3 slice at 50% axial chord of the stator tip. The vortex at the inlet of gap on the blade PS side was the separated vortex (SV), and the vortex near the blade SS in stator passage was the TLV. By comparing the conditions with and without suction on the hub endwall, it could be found that the two-dimensional streamlines and entropy distribution of the Slot SD scheme on this slice had been roughly unchanged, which showed that the downstream suction would not have a significant impact on the upstream flow field. With the Slot SU scheme, the core of TLV was moved toward the stator blade SS and was closer to the hub endwall, which indicated that the upstream suction could restrain the development of TLV in both circumferential and spanwise directions, thereby reducing the strength of the TLF and TLV and improving the compressor aerodynamic performance. The Slot LB scheme had no obvious structure of the leakage vortex in this slice, but there was a structure of the passage vortex (PV) marked by a black ellipse in the top right figure, and the value of entropy near the hub endwall was obviously higher than that of original and other two schemes. The results showed that this suction scheme could greatly enhance the strength of the passage vortex while suppressing the leakage vortex, which with the result that the modification of flow field near the end zone was less effective than that of the short slot suction schemes. An explanation would be raised later for this question.

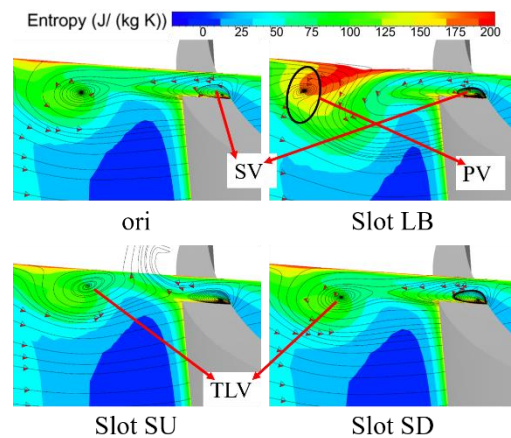


Fig. 11. Streamlines/entropy contour on 50% axial chord slice with the SFR of 0.5%.

Next, we make a detailed analysis of the vortex structure near the hub end region with and without suction. Figure 12 showed the normalized helicity contours of the S3 slices at different axial positions of the original and suction schemes. The normalized helicity H_n is defined as:

$$H_n = \frac{\overline{W} \cdot \overline{\omega}}{|\overline{W}| \cdot |\overline{\omega}|} \quad (1)$$

where \overline{W} and $\overline{\omega}$ denote vectors of relative flow velocity and absolute vorticity, respectively. The normalized helicity H_n is the cosine of the angle

between the velocity vector and the vorticity vector, and its value near vortex core region is close to ± 1 , so that it can be applied to the detection of the vorticity center region. On every slice, the part near the SS of stator blade was the core area of the TLV, whose H_n value was close to +1, and that was connected by the black dotted arrows in the figure to indicate the trajectory of the TLV. The high H_n region near adjacent blade PS was the core of PV.

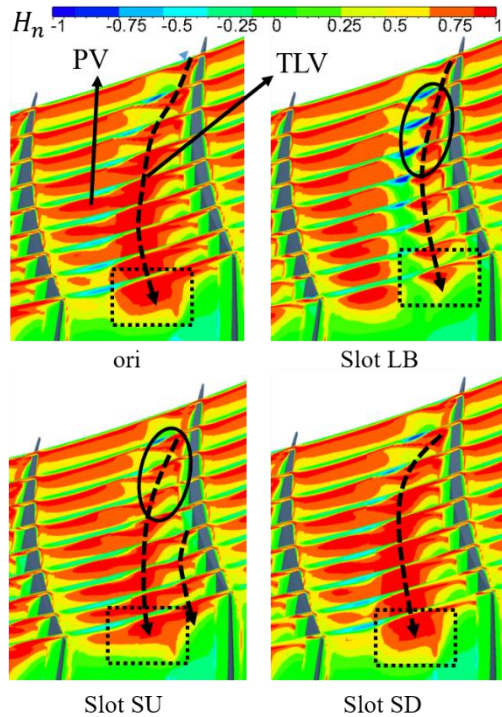


Fig. 12. Normalized helicity on axial slices of the endwall suction with the SFR of 0.5%.

As can be seen from the figure, the TLV began from near the stator blade LE, and its strength and influence range was increased with the flow developing downstream. Similar to Fig.9, the Slot SU scheme had two trajectories of leakage vortex, while the Slot LB scheme failed to identify accurately the trajectory of leakage vortex started at the middle chord because the leakage vortex was too close to the SS of the blade. Compared with the helicity distribution, the suction reduced the spanwise and circumferential range of the high value region, made the core of TLV close to the blade SS, thus reduced the influence range and intensity of the TLV and reduced the flow loss caused by leakage flow. According to the trajectory of the TLV and the regions with high H_n value marked by the black box on the S3 slice near the stator blade TE, the Slot LB scheme had the best control effect on the TLV, while the Slot SD scheme had the worst flow control effect. Because there was a long-term relationship between the passage vortex and the leakage vortex (Zuo *et al.* 2011), the above conclusions could also be obtained indirectly by comparing the development trajectories and influence ranges of the PV. With suction, the TLV was only in the area near the SS of the blade.

Therefore, in the endwall area, the accumulation of low-energy fluid at the blade tip was strengthened. Under the effect of the lateral pressure gradient in the endwall area, the low-energy fluid forming the PV increased, resulting in the increase of the intensity of the hub passage vortex. The effect of PV with stronger intensity than the other two schemes on the flow loss in the tip flow field might be the reason that the Slot LB scheme improved the overall aerodynamic performance of the compressor slightly, although this scheme had the best control effect on TLV. We had given a brief description in the previous paragraph and would further explore and analyze the causes of this result in the following.

In order to describe more intuitively the effect of endwall suction on the structural scale and location of TLV in the rotor passage, the three-dimensional vortex structure under Q criterion is shown in Fig.13, and the structure in this figure was the isosurface of $Q = 5 \times 10^6 s^{-2}$. The Q is defined as:

$$Q = \frac{1}{2} (\Omega_{ij}\Omega_{ij} - S_{ij}S_{ij}) \quad (2)$$

where $\Omega_{ij} = (u_{ij} - u_{ji})/2$ and $S_{ij} = (u_{ij} + u_{ji})/2$ are the spin tensor and strain-rate tensor, respectively. The TLV was shown and marked by the red dotted lines. From the figure, it could be seen that the TLV would aggravate the blocking effect near the end passage and increased the flow loss. With suction, the structure scale of TLV decreased to some extent, and the influence range of TLV of the Slot LB scheme was obviously reduced. There was no obvious boundary between the upstream leakage vortex and downstream leakage vortex with the Slot LB scheme in the upper right figure. At the same time, the development of TLV could also be seen to be suppressed viewed from the changes of the TLV scale in the adjacent passage. The tip leakage vortex in the Slot SU scheme showed a distinct boundary between the upstream leakage vortex and downstream leakage vortex, and the upstream vortex had basically dissipated at the middle chord. Besides, the structure of TLV in the adjacent passage with this endwall suction scheme was not visible in the same view. By comparing the upper right figure with the lower left figure in Fig.13, it was shown that the distribution range in spanwise of the TLV of the Slot SU scheme was wider than that of the Slot LB scheme, but on the other hand, its axial range was smaller. For the Slot SD scheme, the structure of TLV was basically unchanged, but that in adjacent passage decreased slightly.

Through the analysis of the three-dimensional structures of the TLV, one could see that the Slot LB scheme had the largest impact on the diffusion of leakage vortex in spanwise, and the Slot SU scheme had the greatest influence on development in axial direction of leakage vortex near the hub endwall. As previous analysis, the Slot SD scheme had the least influence on the TLF and TLV. Through the analysis of Fig.10, 12 and 13, slotted suction on the hub endwall could modify the flow field near end region by directly affecting the structure of the TLF and TLV. It was different from the control mechanism of

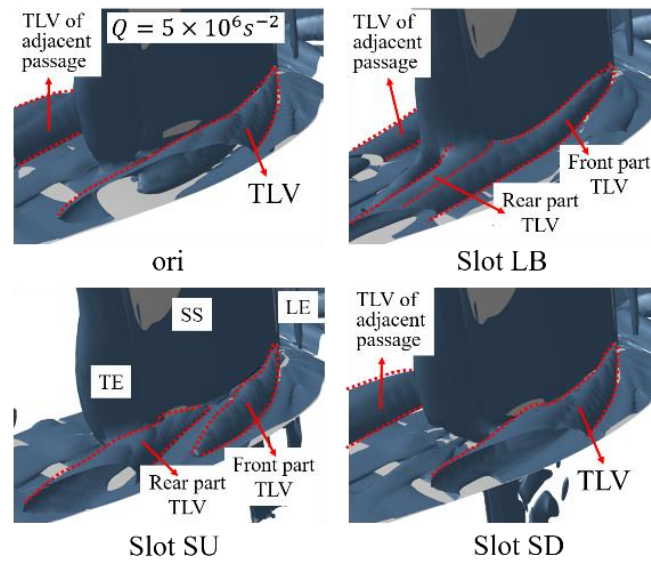


Fig. 13. Q-Isosurface and three-dimensional structures of the TLV.

the circumferential slotted suction scheme on the endwall to improve the compressor performance by affecting the mixing effect of the TLV with the endwall boundary layer and the mainstream (Wang *et al.* 2012; Shi *et al.* 2015b; Lu *et al.* 2017b).

To further explore and quantify the reasons for different flow control effect of the axial position of suction slot on the flow field in the cantilever stator end region, Fig.14 shows the distribution of static pressure coefficient on the surfaces of the stator blade at 3% relative blade height. According to the previous work and related researches (Cao 2014; Perry *et al.* 2017), the endwall suction has little effect on the flow field in the region of middle blade and the gap-free endwall, thereby that was no provided and no further discussed here.

What could we see from the figure was that the three suction schemes adopted in this paper mainly changed the static pressure distribution on the stator blade SS near the hub end, but had little difference on the stator blade PS. The Slot SU scheme was considered first, the static pressure coefficient on the blade SS was lower than that of the original in the range of 15%-35% axial chord length. Then it increased significantly over the original in the range of 35%-60% axial chord length, which was the main effective area for controlling TLF through this suction scheme, and reached the maximum at 45% axial chord length. Lastly, the static pressure on the blade SS decreased slightly over the original after 60% axial chord length. For the Slot SD scheme, the static pressure coefficient on the blade SS was higher than that of the original after 80% axial chord length, but the lifting range was much smaller than that of the Slot SU scheme. It was lower significantly in the range of 40% to 80% axial chord length, and there was no obvious change before 40% axial chord length. In addition, for the Slot LB scheme, the static pressure coefficient on blade SS was higher than that of the original compressor stator blade from the

blade LE to 15% axial chord length. This made the tip load decrease at the stator blade LE, and caused the onset position of the leakage vortex to move downstream. Subsequently, the static pressure coefficient was lower over the original from 15% to 60% axial chord length, moreover, the pressure reduction of this endwall suction scheme was the largest among the three schemes in this range. Finally, the static pressure coefficient was higher again from 60% axial chord length to the blade TE.

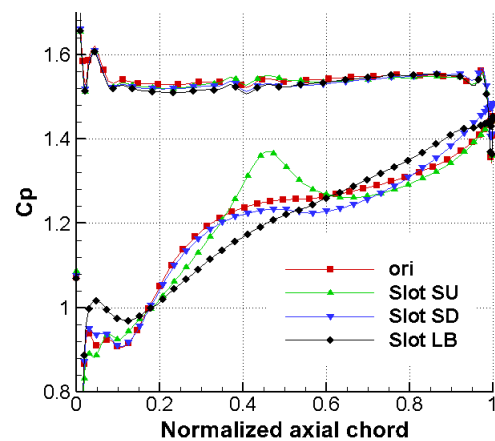


Fig. 14. Static pressure coefficient distribution at 3% span of the stator blade.

The endwall suction increased the static pressure on blade SS in the latter half area covered by suction slot as well as some downstream part of the suction slot by removing the leakage flow near the stator blade SS, which reduced the load of stator blade tip. Thus, the onset position of the TLV was changed and the strength of the TLF and TLV was weakened. The reduction of static pressure on blade SS and the increase of blade loading in the first half area covered by the suction slot as well as the earlier upstream part

of the suction slot were due to the local acceleration effect of the TLF by aspirating some leakage flow. For the Slot SU scheme, the increase of blade loading caused by the decrease of static pressure coefficient on blade SS after 60% axial chord was due to the re-formation of tip leakage vortex in this axial range. Compared with three endwall suction schemes, the Slot SD scheme had the least influence on the blade tip loading, which corroborated with the previous analysis.

Figure 15 and 16 show the distribution of the circumferentially mass-averaged entropy and total pressure ratio of the stator exit along with the relative blade height respectively. The relative blade height in the region below 50% was shown in the figures. According to Yoon's viewpoint (Yoon *et al.* 2015), because the traditional loss coefficient assumed a no-work condition and did not account for the added energy due to rotating surfaces, using entropy was a better way to evaluate the compressor aerodynamic performance, and it was the reason why we chose entropy in this part, too.

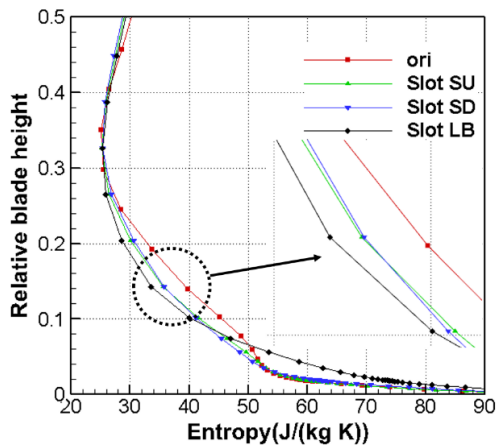


Fig. 15. Circumferentially average entropy distribution of the stator exit.

Figure 15 showed that the endwall suction changed the distribution of entropy near the gap end, which affected the flow loss in the area below 30% relative blade height. Entropy values of the Slot SU and Slot SD schemes in this range had been reduced effectively, which indicated that both schemes could effectively reduce the blocking effect and modify the flow field in the end zone. There was a little difference in the distribution of the entropy between two short slot schemes, except that the entropy of the Slot SU scheme was slightly smaller in the range of 14%-30% relative blade height, while that in the range below 14% relative blade height was opposite. It was because that the upstream suction scheme made the onset position of the TLV moved to the downstream, which greatly shortened the axial development range and reduced the radial influence range of the TLV. As a result, the total pressure loss in the higher relative blade height area was smaller. The TLV of the Slot SU scheme re-formed downstream of the suction slot were stronger than that of the Slot SD scheme suctioned on the

downstream of the stator hub, thus the flow loss near endwall area of the lower relative blade height was slightly higher than that of the Slot SD scheme.

For the Slot LB scheme, the entropy value was lower than that of the original in the range of 6%-30% relative blade height and that was lower over the short slot suction schemes on the same time, which was caused by the movement toward downstream of the onset position of TLV and the weakness of TLV intensity. In the area below 6% relative blade height, the entropy was higher, which was obviously different from the entropy distribution of the short slot suction schemes. Combining with Fig.11 and Fig.12, the main reason for the increase of flow loss near endwall was the large increase of the passage vortex intensity and influence range.

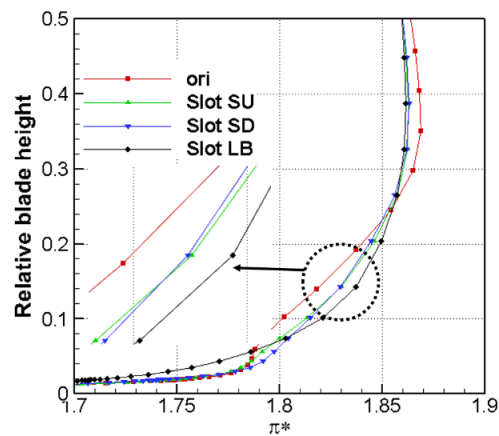


Fig. 16. Radial Distribution of the total pressure ratio of the stator exit.

From Fig.16, the impact of the axial position of suction slot on the distribution of pitchwise mass-averaged total pressure ratio at stator outlet along the spanwise was consistent with the distribution of entropy in the area below 26% relative blade height. However, in the mid-span range, the endwall suction would reduce the total pressure ratio, which meant that the stator turbocharging was redistributed along the spanwise, and the stator blade tip region undertook a larger turbocharging task.

Finally, the problems that may affect the actual effect of the boundary layer suction technique in the engineering application of the real engine are discussed. The suction technique can be combined with the engine bleed air technique, to improve the quality of the internal flow field of the compressor while satisfying the bleed air demand of the air system, maximizing the profit of suction, and then improve the overall performance of the aero engine. However, at the same time, some technical barriers of the suction technique also hinder the practical engineering application effect of this technology.

Opening suction slots or suction holes on the endwall may cause the problem of compressor structure and strength. This problem not only needs to be considered in the aerodynamic design of the compressor, but also needs comprehensive and

careful strength calculation and check. Only when the strength of the suction scheme meets the safety requirements of the engine, the suction technique can be further investigated and evaluated. Taking current research as an example, from Fig.8, the flow control effect of the full chord slot scheme shows a clear advantage in improving the overall performance of the compressor under a large suction flow rate. However, considering the damage caused by the suction slot to the strength of the endwall and the economic performance, more attention was paid to the suction schemes with short slot that have less impact on the strength of the compressor.

In addition, the suction technique requires the introduction of related adsorption power equipment and control mechanisms, which will inevitably increase the weight of the engine and the complexity of the work, and reduce the benefits of the suction control method. Therefore, in the future research, it is necessary to further develop the integrated design of the internal suction flow path layout and engine air system, develop the adsorption power equipment and control mechanism with lighter weight and more reliable performance, and reduce the use cost of the active control method as much as possible. Only in this way, the suction technique can be applied in the actual engine earlier and better.

5. CONCLUSION

In this paper, the impact of the axial position of endwall suction slot on the tip leakage flow in the cantilever stator was studied numerically. The flow control effect of three endwall suction schemes on the tip leakage flow behaviors inside and the corresponding mechanism of modifying the flow field near the hub endwall was analyzed in detail. The main conclusions could be drawn as follows:

- (1) The endwall flow suction can control the flow loss and blocking effect in the end region by directly affecting the structure of the tip leakage vortex. The improvement of compressor performance by slot suction on the hub endwall increased with the increase of suction flow rate, and the endwall suction slot would interfere with the clearance flow field. In the case of small suction flow rate, for example, 0.5%, the short slot schemes can improve the overall efficiency of the compressor by about 0.5%, which is more advantageous than the long slot scheme in improving efficiency, and the overall efficiency improvement of the latter is about 0.3%. The advantage of the long slot scheme in flow control is reflected in the case of large suction flow rate, that is, 1.0%, which may improve the overall efficiency of the compressor by about 0.96%.
- (2) For the boundary layer suction schemes on hub endwall with full chord slot and upstream short slot, the main way to control the tip leakage flow is to make the onset position of the hub leakage vortex move downstream, thereby reduce the strength and influence range of the leakage vortex, and reduce the compressor total pressure

loss. For the aspiration strategy by downstream short slot on the stator hub endwall, the major control mechanism on the leakage flow of cantilever stator is to attenuate the hub leakage vortex by suppressing the downstream development in flow direction and the diffuseness in spanwise. Thus, the aerodynamic performance of the compressor is improved.

- (3) For three aspiration schemes by flow direction slot set up on the hub endwall, the Slot SU scheme has the greatest influence on the shape and scale of the hub leakage vortex as well as the loading of the stator blade tip, thus which is the best effective on modifying the overall flow field in the end zone. The Slot SD scheme has little effect on the structure of tip leakage vortex, but it can also control the leakage flow near the downstream endwall by reducing the blocking effect of cantilever stator passage. The Slot LB scheme also has an excellent control effect on tip leakage vortex, but at the same time, the dramatic increase of intensity of passage vortex makes the modification effect of flow field greatly discounted by this scheme.

ACKNOWLEDGMENTS

This paper is supported by National Natural Foundation of China (Project No: 51676162, 51790512) and National Science and Technology Major Project (Project No: 2017-II-0001-0013), these supports are gratefully acknowledged.

REFERENCES

- An, G., Y. Wu, J. Lang, Z. Chen and B. Wang (2018). Numerical Investigations into the Origin of Tip Unsteadiness in a Transonic Compressor. *Journal of Applied Fluid Mechanics* 11(4), 1133-1141.
- Cao, Z. (2014). *Investigation of Boundary Layer Suction on the Influence of Flow Control and Performance of Axial Flow Compressor*. Ph.D. thesis, Northwestern Polytechnical University.
- Chen, S., S. Sun, Y. Lan and S. Wang (2013). The effect of different clearance geometry configurations on aerodynamic performance in a high-load compressor cascade. *Proceedings of the Institution of Mechanical Engineers, Part G: Journal of Aerospace Engineering* 228(8), 1425-1433.
- Denton, J. D. (1993). Loss Mechanisms in Turbomachines. *Journal of Turbomachinery* 115(4), 621-656.
- Denton, J. D. (1997). Lessons from rotor 37. *Journal of Thermal Science* 6(1), 1-13.
- Du, J., F. Lin, H. Zhang and J. Chen (2010). Numerical Investigation on the Self-Induced Unsteadiness in Tip Leakage Flow for a Transonic Fan Rotor. *Journal of Turbomachinery* 132(2), 021017.

- Gao, J., W. Fu, F. Wang, Q. Zheng, G. Yue and P. Dong (2017). Experimental and numerical investigations of tip clearance flow and loss in a variable geometry turbine cascade. *Proceedings of the Institution of Mechanical Engineers, Part A: Journal of Power and Energy* 232(2), 157-169.
- Glanville, J. P. (2001). Investigation into Core Compressor Tip Leakage Modelling Techniques Using a 3D Viscous Solver. *ASME 2001-GT-0336*.
- Gottschall, M. and K. Vogeler (2013). Vortex development induced by part gap geometry and endwall configurations for variable stator vanes in a compressor cascade. *Proceedings of the Institution of Mechanical Engineers, Part A: Journal of Power and Energy* 227(6), 692-702.
- Gottschall, M., R. Mailach and K. Vogeler (2012). Penny Gap Effect on Performance and Secondary Flowfield in a Compressor Cascade. *Journal of Propulsion and Power* 28(5), 927-935.
- Gümmer, V., M. Goller and M. Swoboda (2008). Numerical Investigation of End Wall Boundary Layer Removal on Highly Loaded Axial Compressor Blade Rows. *Journal of Turbomachinery* 130(1), 011015.
- Guo, S., S. Chen, Y. Song, Y. Song and F. Chen (2010). Effects of Boundary Layer Suction on Aerodynamic Performance in a High-load Compressor Cascade. *Chinese Journal of Aeronautics* 23(02), 179-186.
- Inoue, M. and M. Kuroumaru (1989). Structure of Tip Clearance Flow in an Isolated Axial Compressor Rotor. *Journal of Turbomachinery* 111(3), 250-256.
- Inoue, M., M. Furukawa, K. Saiki and K. Yamada (1998). Physical Explanations of Tip Leakage Flow Field in an Axial Compressor Rotor. *ASME 98-GT-91*.
- Kang, S. and C. Hirsch (1994). Tip Leakage Flow in Linear Compressor Cascade. *Journal of Turbomachinery* 116(4), 657-664.
- Lee, G. H., J. I. Park and J. H. Baek (2004). Performance Assessment of Turbulence Models for the Quantitative Prediction of Tip Leakage Flow in Turbomachines. *ASME GT2004-53403*.
- Lin, A., Q. Zheng, Y. Jiang, X. Lin and H. Zhang (2019). Sensitivity of air/mist non-equilibrium phase transition cooling to transient characteristics in a compressor of gas turbine. *International Journal of Heat and Mass Transfer* 137, 882-894.
- Liu, B., G. An, X. Yu and Z. Zhang (2016b). Quantitative evaluation of the unsteady behaviors of the tip leakage vortex in a subsonic axial compressor rotor. *Experimental Thermal and Fluid Science* 79, 154-167.
- Liu, B., X. Mao, P. Zhang, H. Cheng and X. Wu (2016a). Research on Effects of Tip Clearance on Performance of a Contra-Rotating Compressor. *Journal of Propulsion Technology* 37(05), 815-825.
- Loughery, R. J., R. A. Horn and P. C. Tramm (1971). Single stage experimental evaluation of boundary layer blowing and bleed techniques for high lift stator blades. *NASA Contractor Report No. CR-54573*.
- Lu, H., X. Han, S. Guo, A. Wang and K. Zhong (2017b). Numerical simulation of aerodynamic performance of transonic compressor rotor with circumferential slot boundary layer suction at different locations. *Journal of Harbin Engineering University* 38(12), 1877-1883.
- Lu, H., X. Han, Y. Zhang, Y. Wang, K. Zhong and S. Guo (2017a). Numerical simulation of transonic compressor rotor performance affected by the casing circumferential groove suction. *Journal of Engineering Thermophysics* 38(06), 1191-1195.
- Lu, H., Y. Zhang, D. Kang and B. Liu (2016). Investigation of boundary layer suction on compressor cascade with tip clearance. *Journal of Engineering Thermophysics* 37(02), 277-284.
- Mao, X., B. Liu and H. Zhao (2019). Effects of tip clearance size on the unsteady flow behaviors and performance in a counter-rotating axial flow compressor. *Proceedings of the Institution of Mechanical Engineers, Part G: Journal of Aerospace Engineering* 233(3), 1059-1070.
- Mao, X., B. Liu and T. Tang (2017). Effect of casing aspiration on the tip leakage flow in the axial flow compressor cascade. *Proceedings of the Institution of Mechanical Engineers, Part A: Journal of Power and Energy* 232(3), 225-239.
- Mao, X., B. Liu and T. Tang (2018a). Control of Tip Leakage Flow in Axial Flow Compressor Cascade by Suction on the Blade Tip. *Journal of Applied Fluid Mechanics* 11(1), 137-149.
- Mao, X., B. Liu, R. Abdul and H. Zhao (2018b). Numerical investigation into the effects of casing aspiration on the overall performance and flow unsteadiness in a counter-rotating axial flow compressor. *Aerospace Science and Technology* 78, 671-681.
- Perry, A. T. and P. J. Ansell (2017). Crossflow Fan Power Requirements for Boundary-Layer Suction in Transonic Flow. *Journal of Aircraft* 54(3), 1217-1220.
- Reid, L. and R. D. Moore (1978). Performance of a Single- Stage Axial-Flow Transonic Compressor with Rotor and Stator Aspect Ratios of 1.19 and 1.26, Respectively, and with Design Pressure Ratio of 1.82. *NASA TP-1338*.
- Shi, L., B. Liu, X. Wu, Z. Na and P. Zhang (2015b). Numerical analysis and experimental research

- of shroud casing boundary layer removal on a counter-rotating compressor. *Acta Aeronautica et Astronautica Sinica* 36(9), 2968-2980.
- Shi, L., B. Liu, Z. Na, X. Wu and X. Lu (2015a). Experimental investigation of a counter-rotating compressor with boundary layer suction. *Chinese Journal of Aeronautics* 28(4), 1044-1054.
- Storer, J. A. and N. A. Cumpsty (1990). Tip Leakage Flow in Axial Compressors. *Journal of Turbomachinery* 113(2), 252-259.
- Suder, K. L. (1998). Blockage Development in a Transonic, Axial Compressor Rotor. *Journal of Turbomachinery* 120(3), 465-476.
- Van Zante, D. E., A. J. Strazisar, J. R. Wood, M. D. Hathaway and T. H. Okiishi (2000). Recommendations for Achieving Accurate Numerical Simulation of Tip Clearance Flows in Transonic Compressor Rotors. *NASA/TM—2000-210347*.
- Vo, H. D., C. S. Tan and E. M. Greitzer (2008). Criteria for Spike Initiated Rotating Stall. *Journal of Turbomachinery* 130(1), 011023.
- Wang, Y., N. Niu, S. Ren and L. Zhao (2012). Comparing Effects of Blade Surface with Those of End-Wall Boundary Layer Suction (BLS) on Stability of Transonic Compressor. *Journal of Northwestern Polytechnical University* 30(02), 251-255.
- Wu, Y., G. An and B. Wang (2019). Numerical investigation into the underlying mechanism connecting the vortex breakdown to the flow unsteadiness in a transonic compressor rotor. *Aerospace Science and Technology* 86, 106-118.
- Yoon, S., R. Selmeier, P. Cargill and P. Wood (2015). Effect of the Stator Hub Configuration and Stage Design Parameters on Aerodynamic Loss in Axial Compressors. *Journal of Turbomachinery* 137(9), 091001.
- Zuo, Z., Y. Zhu, D. Zhang and C. Tan (2011). Numerical investigation of the stator hub gap effects on aerodynamic performance of a high-pressure compressor. *Journal of Propulsion Technology* 32(03), 329-333+338.